The Shortest path synthesis for non-holonomic robots moving forwards

Xuân-Nam Bui, Philippe Souères, Jean-Daniel Boissonnat, Jean-Paul Laumond

INRIA

INSTITUT NATIONAL DE RECHERCHE EN INFORMATIQUE ET EN AUTOMATIQUE

The Shortest Path Synthesis for Non-holonomic Robots Moving Forwards

XUÂN-NAM BUI PHILIPPE SOUÈRES

JEAN-DANIEL BOISSONNAT JEAN-PAUL LAUMOND

N° 2153

Décembre 1993

PROGRAMME 4

Robotique,
image
et vision

ISSN 0249-6399

INRIA
SOPHIA ANTIPOLIS

The Shortest Path Synthesis for Non-holonomic Robots Moving Forwards

Xuân-Nam BUI Philippe SOUÈRES *
Jean-Daniel BOISSONNAT Jean-Paul LAUMOND *

Programme 4 — Robotique, image et vision
Projet Prisme

Rapport de recherche n ° 2153 — Décembre 1993 — 33 pages

Abstract: We calculate the partition of the configuration space $\mathbb{R}^2 \times \mathcal{S}^1$ of a car-like robot, only moving forwards, with respect to the type of the length optimal paths. This kind of robot is subject to kinematic constraints on its path curvature and its orientation. Starting from the results on shortest paths by [Dub57] and [BCL92], we give new optimality conditions on these paths, and compute the partition for any horizontal plane of the configuration space.

Key-words: Optimal control, Synthesis problem, Non-holonomic robot, Bounded radius of curvature, Dubins shortest paths

(Résumé : tsvp)

*LAAS
7 avenue du Colonel Roche – 31077 Toulouse
Phone : +33 61 33 63 47 – Fax : +33 61 33 64 55
E-mail : soueres, jpl@laas.fr

This work is partly supported by Esprit Project PROMotion 6546

Synthèse des Plus courts Chemins pour un Robot Non-holonome se Déplaçant en Marche Avant

Résumé : Nous calculons la synthèse pour le problème d'optimisation de la longueur des trajectoires à courbure minorée, d'un robot non-holonome de type voiture, ne se déplaçant qu'en marche avant. Cette synthèse consiste en la partition de l'espace des configurations $\mathbb{R}^2 \times \mathcal{S}^1$ du robot, en fonction des 6 types de chemins optimaux. Nous partons pour cela, des résultats antérieurs de [Dub57] et [BCL92], pour donner de nouvelles conditions nécessaires d'optimalité et calculons la partition de chaque plan horizontal de l'espace des configurations assimilé à $\mathbb{R}^3$.

Mots-clé : Contrôle optimal, Synthèse, Robot non-holonome, Courbure majorée, Plus courts chemins de Dubins

Contents

1 Introduction

We focus here on completing the study on shortest paths for car-like robots which can only move forwards in a plane free of obstacles. These robots are constrained to follow trajectories with bounded curvature (the radius of curvature must be greater than a constant denoted ρ) and their orientation θ is linked to the derivative of the position of a reference point $\mathcal{O}(x, y)$ on the robot, by a differential equation which is not directly integrable (the robot is non-holonomic) :

$$\dot{x} \sin\theta - \dot{y} \cos\theta = 0$$

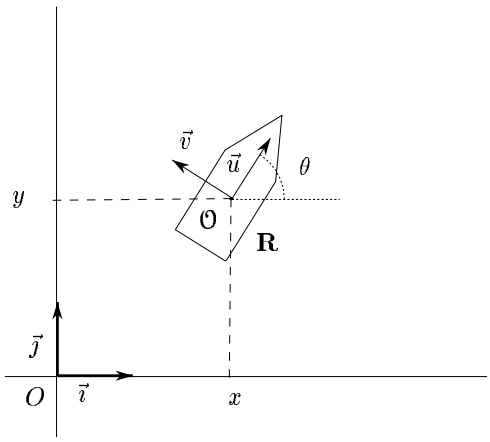

Figure 1: The non-holonomic robot

Shortest paths for such robots have first been studied by L. E. Dubins in 1957 [Dub57], who proved that a shortest path is to be found among a finite set of paths, six to be precise. Assuming that there is no slipping of the wheels and the robot speed is constant equal to 1, its kinematic model is then the following :

$$\begin{pmatrix} \dot{x} \\ \dot{y} \\ \dot{\theta} \end{pmatrix} = \begin{pmatrix} \cos\theta \\ \sin\theta \\ \kappa/\rho \end{pmatrix} \tag{1}$$

where (x, y) are the coordinates of a reference point on the robot, θ the orientation of the robot and κ is the only control parameter, verifying $|\kappa| \leq 1$. From the automatics point of view, these robots are completely controlable, so that it makes sense to study the synthesis problem.

Thus, our aim is to show that it is possible to compute the synthesizing function of this optimality problem, which consists in associating to each point

(x, y, θ) in the configuration space $\Omega = I\!R^2 \times \mathcal{S}^1$ a unique type of shortest path starting at the origin $(0, 0, 0)$ and ending at this configuration. We then obtain a partition of Ω with respect to the six different types of shortest path.

This paper is articulated as follows. First we will present some recent related works, and recall the results of Dubins on shortest paths. Then we will use tools from optimal control theory and geometry, to prove some symmetry properties in the synthesizing function and new optimality conditions on the shortest paths. Finally we will compute the synthesis, with respect to the orientation θ of the final configuration. Hence we will obtain a partition of the parametric plane $P_\theta = I\!R^2 \times \{\theta\}$. But since θ can vary freely in $\mathcal{S}^1$, we also have the partition of the whole configuration space Ω.

2 Previous results

2.1 Related work

A similar work has been done already for the Reeds and Shepp mobile robot. This robot has the same characteristics but moreover, it is allowed to make manœuvres. Reeds and Shepp approached first the problem of shortest paths for such robots in [RS90]. As in Dubins's case, they found a finite sufficient family of types of paths, consisting of at most five parts, either arcs of circle of radius ρ or straight line segments, and at most two manœuvres. This result has been proved again by Sussman and Tang in [ST91], and by Boissonnat, Cérézo and Leblond in [BCL92], using the Maximum Principle of Pontryagin [PBGM62], a well-known tool in optimal control theory. Finally, Souères and Laumond refined the sufficient family of paths, and achieved the study of the synthesis problem for those robots in [SL93], emphasizing the properties of the associated metric. We will see that in our case, some parts of the work, despite of the great similarity, have been found to be more complex, because of the absence of a metric.

2.2 Dubins shortest paths

We recall that a *configuration* is the triplet $\omega = (x, y, \theta)$ defining the position and the orientation of the robot in the plane and the *configuration space* is $\Omega = I\!R^2 \times \mathcal{S}^1$. For such robots, it has been proved, first in [Dub57] and more recently in [BCL92], that for given initial and final configurations in an obstacle-free environment, the shortest path exists and is among six types of paths, consisting of at most three parts which are either arcs of circles of radius ρ (denoted

C), or straight line segments (denoted S). An arc of circle C can be followed in two oppposite directions, either clockwise (then the arc C will be denoted R for "right-arc") or counterclockwise (the arc will be denoted L for "left-arc"). Thus we can classify the six types of shortest paths into two families, illustrated in Figure 2 :

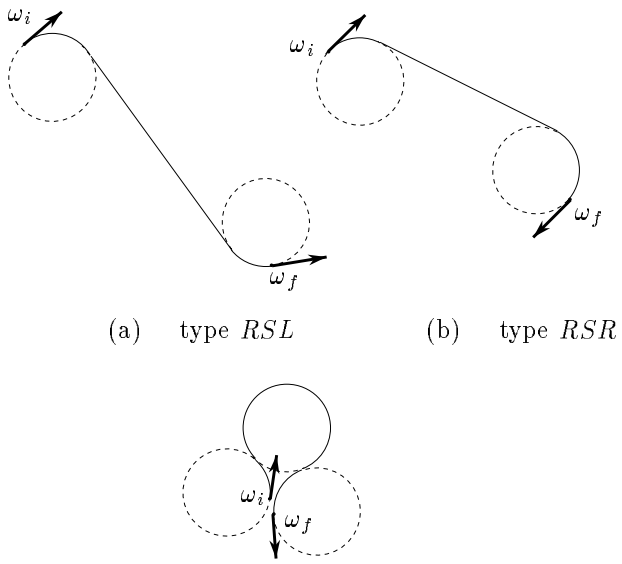

(a) type RSL (b) type RSR

(c) type LRL

Figure 2: Examples of Dubins shortest paths

- Family CCC includes 2 types

  type LR_vL and type RL_vR

  where v is the angle of the intermediate arc, verifying $v > \pi$.

- Family CSC includes 4 types

  type LSL and type RSR

  type LSR and type RSL

3 Synthesis

The criterion to be optimized is the length of the paths, or the time since the speed of the robot is constant. The synthesis of our optimization problem is then to determine for each configuration ω of Ω the shortest path from the origin $\omega_0 = (0,0,0)$ to ω. We must notice that in our particular case, as the robot only moves forward, the problem is not symmetric : if two configurations ω_1 and ω_2 are given, the shortest path from ω_1 to ω_2 is in most cases different from the shortest one from ω_2 to ω_1. That is why the length of the shortest path does not define a metric on Ω.

To solve the synthesis problem, we will first show the existence of symmetries in the configuration space and prove some new necessary conditions of optimality for the types of paths. Using these results, we will be able to work in $\mathbb{R}^2 \times [0,\pi]$ instead of $\mathbb{R}^2 \times \mathcal{S}^1$. Then, to simplify the analysis, we will compute the domains of potential optimality for Dubins paths in a parametric plane P_θ, that is for final configurations with the same orientations θ. The partition of P_θ will then be obtained after discussing the real optimality of the paths in the domain intersections. The partition of Ω will be simply the superposition of all partitions of the planes P_θ, for $\theta \in [0, 2\pi[$.

3.1 Symmetry properties

In [SL93], it is shown that each plane P_θ has two axes of symmetry, that reduces the study to a quarter of the plane, and also the number of shortest path types to consider. Here we will see that there exists only one axis of symmetry and that the number of types to study will only be decreased by one.

Lemma 3.1 *The straight line Δ_θ of orientation $\frac{\theta}{2}$ passing through the origin is an axis of symmetry of the partition of P_θ : if M is a point in P_θ and γ is a shortest path leading to the configuration (M,θ), if M' is the symmetric of M with respect to Δ_θ, then there exists an optimal path γ', isometric to γ, leading to the configuration (M',θ).*

Proof : Let us consider Figure 3. Point M' is obtained after three rigid transformations :

- The symmetry s_{Oy} of vertical axis Oy maps triangle OM_1P_1 onto triangle OMP.
- The translation $t_{\overrightarrow{M_1O}}$ of vector $\overrightarrow{M_1O}$ maps triangle M_2OP_2 onto triangle OM_1P_1.

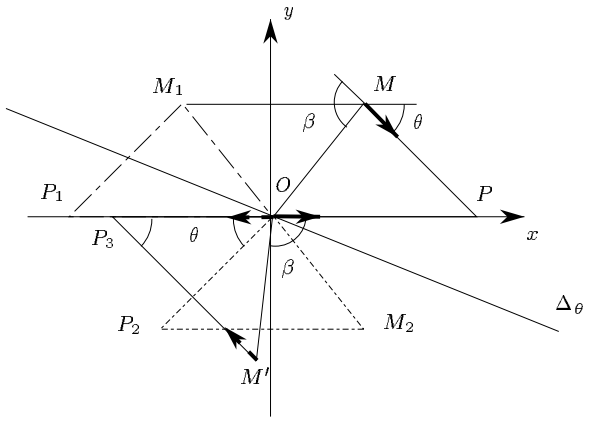

Figure 3: Symmetry w.r.t. Δ_θ

- The rotation r_θ of centre O and angle θ maps triangle $M'OP_3$ onto triangle M_2OP_2.

Thus M' is the image of O by the isometric transformation $r_\theta \circ t_{\overrightarrow{M_1O}} \circ s_{Oy}$, and so is path γ' isometric to path γ, as illustrated in Figure 4.

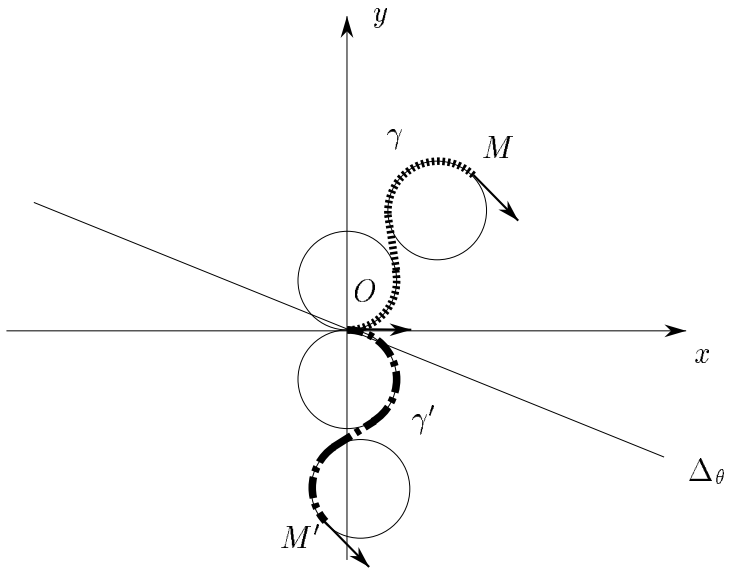

Figure 4: Path γ is of type LSR and path γ' is of type RSL

let us prove that M' can also be obtained as the symmetric of point M by the symmetry of axis Δ_θ. Indeed, we have the following relation :

$$\widehat{MOM'} = \widehat{POM'} - \widehat{POM}$$

So the bisector axis of angle $\widehat{MOM'}$ is equal to :

$$\widehat{POM} + (\widehat{POM'} - \widehat{POM})/2 = (\widehat{POM'} + \widehat{POM})/2$$

Moreover, the angles incident at M satisfy the equation :

$$\beta = \widehat{POM'} = -\widehat{POM} + \theta$$

and hence

$$\widehat{POM'} + \widehat{POM} = \theta$$

So we conclude that if there exists an optimal path γ from ω_0 to $\omega = (M, \theta)$, then the isometric transformation defined above maps γ onto another optimal path γ' from ω_0 to $\omega' = (M', \theta)$, where M' is the point symmetric to point M with respect to axis Δ_θ. As we can notice that the orientations of the images of ω_0 and ω by the isometric transformation are opposite to the orientations of ω_0 and ω' (compare Figures 3 and 4), if we consider the path γ as a word made of letters R, L and S, the word of γ' is obtained by reading the word of γ in reverse order. □

This result allows us to restrict our study to a half-plane defined by Δ_θ, and the types of paths covering it, that is types LRL, RLR, LSL, RSR, and either RSL or LSR.

Lemma 3.2 *The symmetry w.r.t. axis Ox changes an optimal path γ leading to the configuration (x, y, θ) into an isometric optimal path γ'' leading to the configuration $(x, -y, -\theta)$.*

Proof : This proof is directly deduced from the properties of the symmetry s_{Ox}. Here the word of γ'' is obtained from the one of γ by changing the L into R and vice versa. □

With this second property, we can restrict the range of θ to the interval $[0, \pi]$, if $\mathcal{S}^1$ is assumed to be the interval $]pi, \pi]$.

3.2 Additional optimality conditions

We can parametrize Dubins paths by three variables representing the lengths of their arcs and segment. An upper bound on the length of the arcs is obviously 2π. In [BCL92] only the condition ($v > \pi$) on the intermediate arc length of paths CCC is given. We can improve the bounds on the parameters as follows, still using the Maximum Principle of Pontryaguin but also geometrical arguments.

Proposition 3.1 *In an optimal path, the algebraic sum of the arc angles has absolute value less than* 2π.

Thus, any optimal path can be considered as a continuous function from $[0,1]$ *onto* $\mathbb{R}^2 \times [-2\pi, 2\pi]$.

Remark 3.1 We can notice that this property sets an important difference with the case of Reeds and Shepp robot. In our case, any configuration (M,θ), with $\theta \in [0, 2\pi[$, must be considered in two different ways : either as (M,θ) or as $(M,\theta - 2\pi)$ which are the same configurations in the physical space, but not in the configuration space we consider, that is $\mathbb{R}^2 \times [-2\pi, 2\pi]$.

These two possibilities have to be considered only in the case where arcs are not all of the same orientations. Indeed if they are, and if the path from ω_0 to (M,θ) is in $\mathbb{R}^2 \times [-2\pi, 2\pi]$, then the path leading to $(M,\theta-2\pi)$ will not be optimal because it will include an arc of length strictly greater than 2π (since we can turn in only one orientation).

To prove Proposition 3.1, we will successively study each type of Dubins paths.

Lemma 3.3 *Let us consider the path* $C_u C_v C_w$, *where parameters* u, v *and* w *are the angles of each arc of circles. This path can be optimal if*

$$\begin{cases} \pi < v < 2\pi \\ 0 \leq u \leq v \ \ and \ \ 0 \leq w \leq v \\ 0 \leq u < v - \pi \ \ or \ \ 0 \leq w < v - \pi \end{cases}$$

Proof : The first condition on v has been already given in [BCL92].

In this paper, a characteristic straight line D_0 is defined for each optimal path, which supports straight line segments and where inflexion points occur. On one side of this line the path turns clockwise, and on the other side, counterclockwise. Thus if $u > v$, the arc of length u crosses the line D_0, which is not possible.

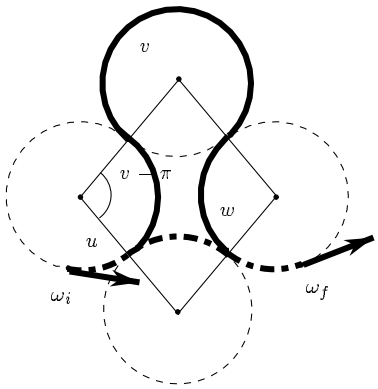

Figure 5: Non optimal CCC paths

For the last condition, suppose that the contrary is true : $u \geq v - \pi$ and $w \geq v - \pi$. Thus there exists another circle tangent to the two extremal arcs, symmetric w.r.t. the segment joining their centres to the circle supporting the intermediate arc. Then on this circle we consider the arc γ of length $2\pi - v < v$ in order to build a shorter path (see Figure 5) : the first arc shortened to length $u - v + \pi$, concatenated to arc γ, which is followed by the last arc shortened to length $w - v + \pi$. But it is not optimal because it belongs to family CCC with an intermediate arc length less than π. □

For paths belonging to family CSC, the case of types RSL and LSR is simple : since each arc has length less than 2π, their algebraic sum is also less than 2π. For types RSR and LSL we need first the following lemma.

Lemma 3.4 *Paths RSR where the sum of the arc lengths is equal to 2π can be replaced by an isometric path LSL, and vice versa.*

Proof : Let us consider two configurations $\omega_i = (M_i, \theta)$ and $\omega_f = (M_f, \theta)$ with $M_i \neq M_f$, as in Figure 6. In both cases, the sum of the arc lengths are equal to 2π. Moreover, the line segments are equal because $N_i N_f P_f P_i$ is a parallelogram. So both paths γ_R and γ_L have same lengths. □

Hence we can state the following lemma, which proves Proposition 3.1 for paths of types RSR and LSL.

Lemma 3.5 *A path $R_u S R_v$ or $L_u S L_v$ can not be optimal if $u + v > 2\pi$.*

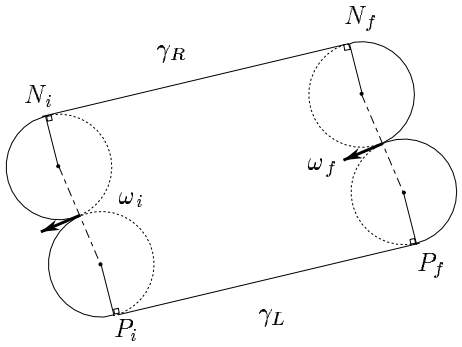

Figure 6: Paths RSR and LSL linking two configurations of same orientations

Proof : If $u+v > 2\pi$, we can find on the first (*resp.* or last) arc a point with the final (*resp.* or initial) orientation. Using the previous lemma, the subpath between these two configurations of same orientations can be replaced by an isometric subpath RSR if it was LSL, and vice versa, to obtain an isometric solution. It is not a Dubins path (see Figure 7), hence it is not optimal. □

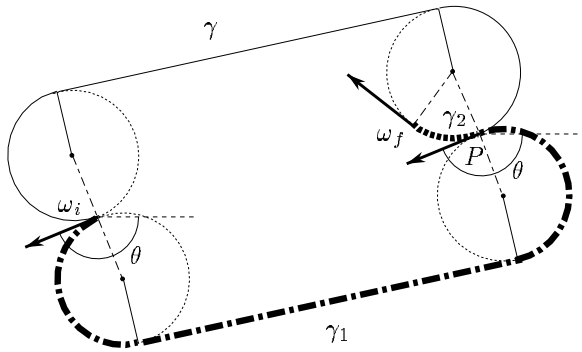

Figure 7: R_uSR_v path with $u + v > 2\pi$

We conclude this section by the following table which sums up the necessary optimality conditions for Dubins paths.

type $C_uC_vC_w$	$v \in]\pi, 2\pi[$ and $u, w \in [0, v]$ and $0 \leq u < v - \pi$ or $0 \leq w < v - \pi$
type $R_vS_sR_u$ or $L_vS_sL_u$	$u, v \in [0, 2\pi[$ and $u + v \leq 2\pi$
type $R_vS_sL_u$ or $L_vS_sR_u$	$u, v \in [0, 2\pi[$

3.3 Domains of each type of path

With the previous symmetry properties, we can restrict our study to all Dubins paths except LSR, in the inferior half-plane of P_θ defined by Δ_θ and with $\theta \in [0, \pi]$. But the figures will show results for the whole plane P_θ, and all the paths.

Each domain is computed in the same way. The control parameter κ introduced in system (1) is known on each part of a Dubins path : it is equal to 1 along an arc L, -1 along an arc R, and 0 along a straight line segment. So we can compute the parametric equations of the points reached from ω_0 with any type of path, by integrating the differential system (1) on each part with the appropriate value of κ. Since we compute the restriction of the domains to the plane P_θ, each path is now parametrized by only two independant parameters, and no more three because those three are linked to θ by a linear equation. First, we need some definitions (see Figure 8).

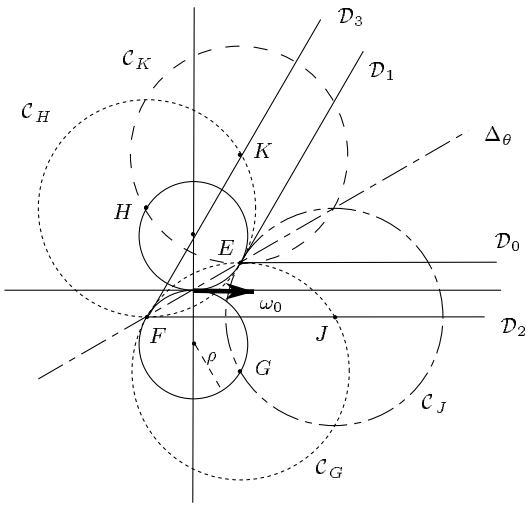

Figure 8: Particular points, lines and circles

- E is the point $(\rho \sin\theta, \rho - \rho\cos\theta)$.
- G is the point $(\rho \sin\theta, -\rho - \rho\cos\theta)$.
- F (*resp.* H) is the point symmetric to E (*resp.* G) w.r.t. the origin O.
- J (*resp.* K) is the point symmetric to H (*resp.* G) w.r.t. point E.
- D_0 (*resp.* D_1) is the ray from E towards positive x-coordinates, of orientation 0 (*resp.* θ).

* D_2 (*resp.* D_3) is the ray from F parallel to D_0 (*resp.* D_1).
* we denote $\mathcal{C}_P$ the circle (or the disc) of centre the generic point P and radius 2ρ.

3.3.1 LSL domain

We denote $L_v S_s L_u$ a generic path of type LSL. The parameters satisfy the relation $u + v = \theta$. If we keep (v, s) as independant parameters, the optimality conditions then consist in : $u, v \geq 0$ and $u + v \leq 2\pi$.

Following the first arc, the reference point $\mathfrak{O}$ reaches the point of coordinates :

$$\begin{cases} \rho \sin v \\ \rho - \rho \cos v \end{cases}$$

Then follows line segment S_s, and the point reached is :

$$\begin{cases} \rho \sin v & +s \cos v \\ \rho - \rho \cos v & +s \sin v \end{cases}$$

Finally, after last arc $L_{u=\theta-v}$, $\mathfrak{O}$ is on the point defined by :

$$\begin{cases} \rho \sin v & +s \cos v & +\rho \sin\theta - \rho \sin v \\ \rho - \rho \cos v & +s \sin v & +\rho \cos v - \rho \cos\theta \end{cases}$$

These coordinates can be simplified, so that we obtain the LSL domain as the set of points M_{LSL} of coordinates :

$$M_{LSL} \begin{pmatrix} \rho \sin\theta & +s \cos v \\ \rho - \rho \cos\theta & +s \sin v \end{pmatrix} \quad \text{with} \quad \begin{cases} v \in [0, \theta] \\ s \in I\!R^+ \end{cases} \tag{2}$$

This domain is shown on Figure 9. As in [SL92], it is stratified by the iso-parametric curves as follows. When v is fixed, s can describe $I\!R^+$ and point M_{LSL} follows the half-line with orientation $\tan v$ and starting at point E. Reciprocally, when s is fixed and v varies within range $[0, \theta]$, point M_{LSL} describes an arc of circle of centre E and radius s. These curves are also iso-distance curves for this type of Dubins path : on such a circle, v and s are fixed, so are $u = \theta - v$ and the path length which is equal to $\rho v + s + \rho u$.

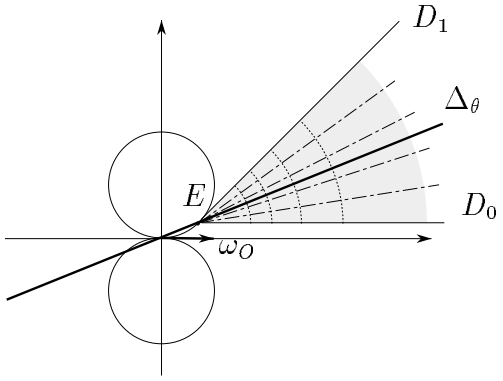

Figure 9: LSL domain

3.3.2 RSR domain

The calculations are similar to the previous case. We denote $R_v S_s R_u$ the path of type RSR, the parameters satisfying the relation $u + v = 2\pi - \theta$ and the conditions $v \in [0, 2\pi - \theta]$ and $s \in I\!R^+$. Then, the RSR domain is the set of points of coordinates :

$$M_{RSR} \begin{pmatrix} -\rho \sin\theta & +s\cos v \\ -\rho + \rho\cos\theta & -s\sin v \end{pmatrix} \quad \text{with} \quad \begin{cases} v \in [0, 2\pi - \theta] \\ s \in I\!R^+ \end{cases} \tag{3}$$

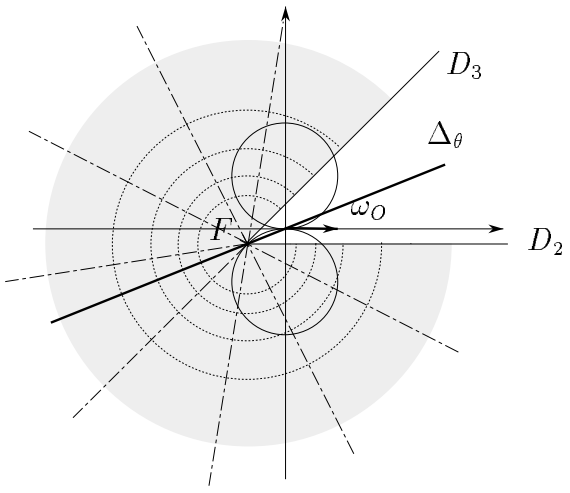

Figure 10: RSR domain

This domain is also stratified by the iso-parametric curves (see Figure 10). They are half-lines of orientation $-\tan v$ and starting at point F, when v is given. But when s is fixed, they are arcs of circle of centre F and radius s. As in the previous case, thes last curves are also iso-distance curves for paths of type RSR.

3.3.3 RSL and LSR domains

These two domains are symmetric with respect to axis Δ_θ. So we will compute the equations of the RSL domain, and the other can be deduced by symmetry. We denote the path $R_v S_s L_u$, where the parameters just have to satisfy $u, v \in [0, 2\pi[$. Then, the set of points reached by $\mathfrak{O}$ describing a path of type RSL has the following parametric equations :

$$M_{RSL} \begin{pmatrix} \rho \sin\theta & +s\cos v + 2\rho \sin v \\ -\rho - \rho\cos\theta & -s\sin v + 2\rho\cos v \end{pmatrix} \quad \text{avec} \quad \begin{cases} v \in [0, 2\pi[\\ s \in I\!R^+ \end{cases} \tag{4}$$

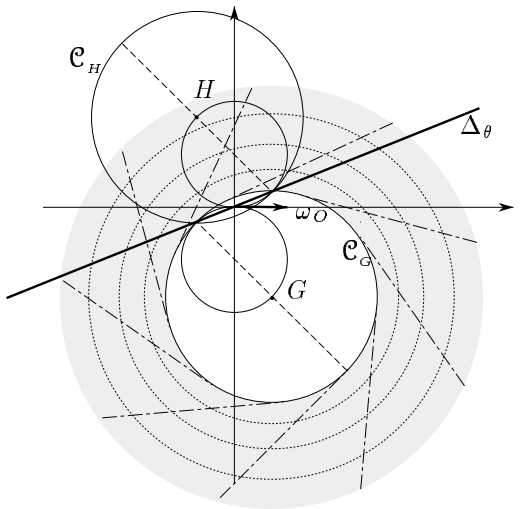

Figure 11: RSL domain

It is the plane P_θ minus the interior of circle $\mathcal{C}_G$. In this case, when v is fixed, point M_{RSL} desribes a half-line tangent to circle $\mathcal{C}_G$, starting from this circle and of orientation $-\tan v$. Reciprocally when s is fixed and v varies in the interval $[0, 2\pi[$, point M_{RSL} describes the circle of centre G and radius $\sqrt{s^2 + 4\rho^2}$.

Remark 3.2 Symmetrically, the LSR domain is the plane P_θ minus the interior of circle $\mathcal{C}_H$.

Iso-distance curves for paths of type RSL

We will prove that these curves are involutes of circle $\mathcal{C}_G$. Let us consider two points M_1 and M_2 on the same iso-parametric curve with s fixed, that is a circle of centre G and radius $\sqrt{s^2+4\rho^2}$. Thus the RSL paths $\gamma_1 = R_{v_1}S_sL_{u_1}$ and $\gamma_2 = R_{v_2}S_sL_{u_2}$ from ω_0 leading respectively to M_1 and M_2, have the same length of line segment. As shown on Figure 12, the difference between the total lengths comes from the arcs, and in this case the sum of the arcs of γ_1 is longer than the one of γ_2. Let us denote $\alpha = v_1 - v_2$ the angle in gray on circle $\mathcal{C}_R$, which is also equal to the difference $u_1 - u_2$. So the diffence of length between γ_1 and γ_2 is $2\rho\alpha$. α is also the angle in gray on circle $\mathcal{C}_G$: the segment of path γ_1 is parallel and equal to segment T_1M_1. This also holds for the segment of path γ_2 and segment T_2M_2. So the angle between segments T_1M_1 and T_2M_2 is α. Then, point M_3 built as the point distant from M_2 by $2\rho\alpha$ and lying on the same line tangent to $\mathcal{C}_G$ as M_2, is such that the path γ_3 of type RSL has the same length as path γ_1. Indeed the arcs of γ_3 and γ_2 are equal, and the segment of γ_3 is equal to $s + 2\rho\alpha$.

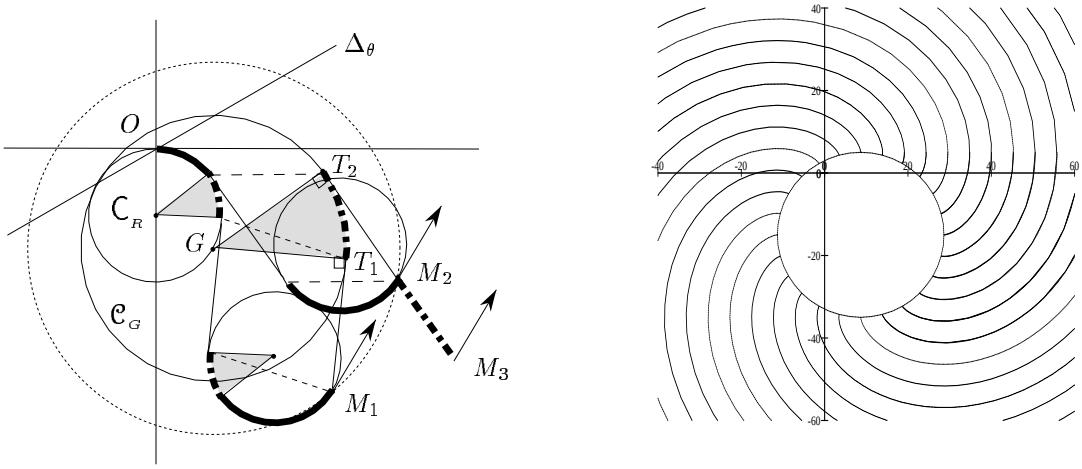

Figure 12: Iso-distance curves for type RSL (on the right for $\theta = \pi/3$)

By definition of an involute[1], M_3 is on the same involute of circle $\mathcal{C}_G$ as M_1. Thus, the iso-distance curves for paths of type RSL are involutes of circle $\mathcal{C}_G$. The minimum length of such paths is θ, corresponding to parameters $(0, 0, \theta)$ and to single point E. We can notice then, that on half-line D_0 the length of RSL

[1] A practical construction of an involute of a circle is the following : it is the curve described by the endpoint of a string that one would wrap or unwrap around the circle.

paths is discontinue : following an involute, the path length makes a jump of $2\pi\rho$, since parameter v equals 0 on and below D_0, and tends to 2π above it.

3.3.4 LRL domain

The path is denoted $L_u R_v L_w$. As noticed in Comment 3.1, we have two possible euqations linking these three parameters to θ : either $u+w-v=\theta$ or $v-u-w=2\pi-\theta$. Associated to the optimality conditions, we get the following variation intervals for the independent parameters u and v that we keep :

- $u+w-v=\theta$ and $u \in]\theta+\pi, 2\pi[$ and $v \in [u, 2\pi[$
  or
  $u \in]\theta, \pi[$ and $v \in [u+\pi, 2\pi[$
- $v-u-w=2\pi-\theta$, $u \in [0, \theta[$ and $v \in [2\pi+u-\theta, 2\pi[$

The parametric equations of points in the LRL domain are then the following :

$$M_{LRL}\begin{pmatrix} \rho\sin\theta & +2\rho\sin(v-u)+2\rho\sin u \\ \rho-\rho\cos\theta & +2\rho\cos(v-u)-2\rho\cos u \end{pmatrix}$$

$$\text{with } \begin{cases} u \in [0,\theta[\\ v \in [2\pi+u-\theta, 2\pi[\end{cases} \text{ or } \begin{cases} u \in [\theta,\pi[\\ v \in [\pi+u, 2\pi[\end{cases} \text{ or } \begin{cases} u \in [\theta+\pi, 2\pi[\\ v \in [u, 2\pi[\end{cases} \tag{5}$$

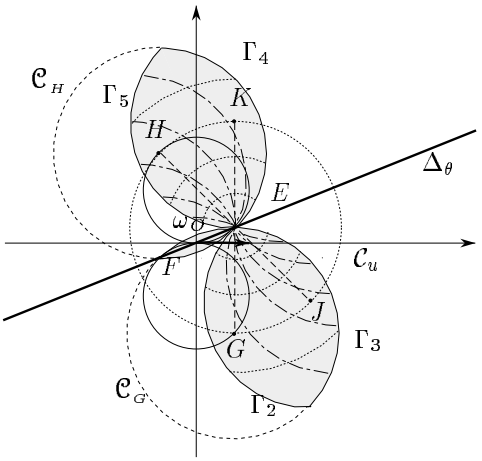

Figure 13: LRL domain

We obtain three subdomains corresponding to those three variation intervals of (u, v). Let us make them clear. But first we can notice that point E is common

to all of them, since it corresponds to the limit $v = 2\pi$, and that if v is fixed, point M_{LRL} describes an arc of circle of centre E and radius $2\rho\sqrt{2-2\cos v}$. These arcs are also iso-distance curves, since when v is fixed, so is the sum $u+w$, hence the path length $\rho\,(u+v+w)$ is constant. We must notice that the path length is inversely proportional to the radius of tose circles.

1. $u \in [0, \theta[$ and $v \in [2\pi + u - \theta, 2\pi[$.

   The corresponding subdomain is the region between two arcs of circle Γ_0 and Γ_1 of radius 2ρ, and respectively of centre G and H (see Figure 14). When u is fixed, the iso-parametric curves are arcs of circles of centre N_u and radius 2ρ, starting at point E. Point N_u is on a circle denoted $\mathcal{C}_u$ of radius 2ρ and its coordinates are $\begin{pmatrix} \rho\sin\theta + 2\rho\sin u \\ \rho - \rho\cos\theta - 2\rho\cos u \end{pmatrix}$.

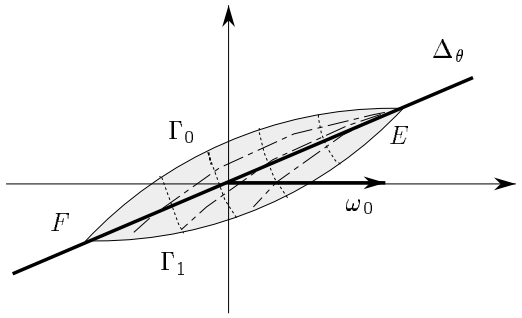

Figure 14: Subdomain corresponding to $u \in [0, \theta[$ and $v \in [2\pi + u - \theta, 2\pi[$

2. $u \in [\theta, \pi[$ and $v \in [\pi + u, 2\pi[$.

   This subdomain is the region delimited by the arcs of circle Γ_2 and Γ_3 of radius 2ρ, and respectively of centre J and G (see Figure 13). When u is given, point M_{LRL} describes an arc of circle of centre N_u.

3. $u \in [\theta + \pi, 2\pi[$ et $v \in [u, 2\pi[$

   We get the symmetric subdomain of the previous one with respect to axis Δ_θ. It is the region between arcs of circle Γ_4 and Γ_5 of radius 2ρ, and respectively of centre H and K (see Figure 13).

3.3.5 *RLR* domain

We denote the path $R_u L_v R_w$, and as in the previous case, two possibilities occur : the parameters satisfy either the equation $u+w-v = 2\pi-\theta$ or $v-u-w = \theta$. But

in fact, the first case gives no solution compatible with the optimality conditions. Just remains the case where $v - u - w = \theta$, either with $u \in]\pi - \theta, 2\pi - \theta[$ and $v \in [u + \theta, 2\pi[$, or $u \in]0, \pi[$ and $v \in [u + \pi, 2\pi[$.

The RLR domain is then the set of points of parametric equations :

$$M_{RLR} \begin{pmatrix} -\rho \sin\theta & +2\rho \sin u & +2\rho \sin(v-u) \\ -\rho + \rho\cos\theta & +2\rho\cos u & -2\rho\cos(v-u) \end{pmatrix} \tag{6}$$

$$\text{with} \quad \begin{cases} u \in]\pi - \theta, 2\pi - \theta[\\ v \in [u + \theta, 2\pi[\end{cases} \quad \text{or} \quad \begin{cases} u \in]0, \pi[\\ v \in [u + \pi, 2\pi[\end{cases}$$

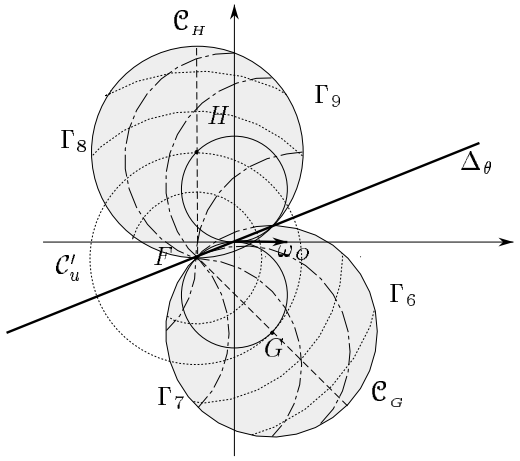

Figure 15: RLR domain

When u is given and v varies, point M_{RLR} describes an arc of circle of radius 2ρ and centre N'_u. This point of coordinates $\begin{pmatrix} -\rho\sin\theta + 2\rho\sin u \\ -\rho + \rho\cos\theta + 2\rho\cos u \end{pmatrix}$ is also on a circle $\mathcal{C}'_u$ of radius 2ρ and centre F (see Figure 15). And when v is fixed, M_{RLR} describes an arc of circle of centre F and radius $2\rho\sqrt{2 - 2\cos v}$. These circles are also iso-distance curves, and the path length, as for type LRL, is inversely proportional to the radius of the circle.

1. $u \in [\pi - \theta, 2\pi - \theta[$ and $v \in [u + \theta, 2\pi[$

   The subdomain is the disc of centre G and radius 2ρ.

2. $u \in [0, \pi[$ and $v \in [u + \pi, 2\pi[$

   This subdomain is symmetric to the previous one with respect to axis Δ_θ, so it is the disc of centre H and radius 2ρ.

Notice that these domains intersect each other and do not partition P_θ (see Figure 16). But they share the same property : they are defined by two parameters, and the iso-parametric curves create two secant foliations of the domain, proving that for any point in the interior of a type domain, there exists a unique shortest path of that type.

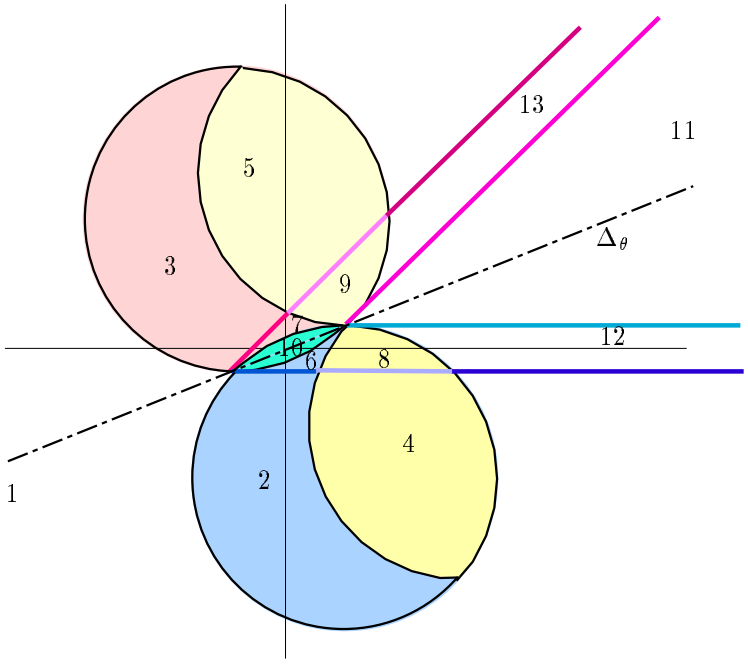

Figure 16: Domain intersections for $\theta = \pi/4$

1	*RSR-RSL-LSR*	11	*LSL-RSL-LSR*
2	*RSR-RLR-LSR*	3	*RSR-RLR-RSL*
4	*RSR-LSR-RLR-LRL*	5	*RSR-RSL-RLR-LRL*
6	*RLR-LSR*	7	*RLR-RSL*
8	*RLR-LRL-LSR*	9	*RLR-LRL-RSL*
10	*RLR-LRL*	12-13	*RSL-LSR*

3.4 Partition of P_θ

We still have to decide what is the type of the optimal path in each region of P_θ covered by more than one domain.

We are sure of the optimality of the whole LSL domain for the LSL type, even if other domains are intersecting it. Indeed, this domain is optimal in the Reeds and Shepp case. As the Dubins sufficient family of types is included in the Reeds and Shepp one (except the CCC paths, which are shortened to $C|C|C$ paths, where the symbol | means a manœuvre), a corresponding optimal region for the Reeds and Shepp case is a fortiori optimal in the Dubins case. So we have to consider the other possibilities of intersection. We will only present here the final equations of the intersection curves, since the method may lead to complex calculations (see [Bui94] for more details).

3.4.1 Intersection RSR / RSL

In the intersection of the two domains, which is the complementary set of the union of the disc $\mathcal{C}_G$ and the internal angular sector defined by the rays D_2 and D_3 (region 1), we have to decide where the types RSR and RSL are optimal. In order to solve this problem, we want to compute the parametric equations of the configurations for which the two types of path reaching them have the same lengths. So we write the equalities of the coordinates and of the lengths, which gives a system of three equations with four variables. We solve it, keeping one variable as a parameter. The set of points where the two paths have the same length is then a curve called $calI_0$ of parametric equations :

$$calI_0 \quad \begin{cases} x = \lambda \cos v + 2\rho \sin v + \rho \sin\theta \\ y = -\lambda \sin v + 2\rho \cos v - \rho \cos\theta - \rho \end{cases}$$

with $\lambda = \frac{\rho(v+\theta-\pi)^2 + 2\rho(\cos(v+\theta)-1)}{\sin(v+\theta)-(v+\theta-\pi)}$, and v is the length of the first arc in the RSL path. This parameter varies in the interval $]\pi-\theta, \pi-\theta+\eta]$, for any $\theta \in [0, \pi[$ and η is the solution of the non-algebraic equation $\cos t = t$.

This curve divides the domains intersection in two sub-domains, and admits as asymptote the line passing through G of orientation θ (see Figure 17). We define the symmetric curve $calI_1$ for the intersection between RSR and LSR.

3.4.2 Intersection RSL / LSR

We use here the results on iso-distance curves for both types of paths to prove that LSR paths are always shorter than RSL paths in region 13, as it is shown in Figure 18. Symmetrically with respect to axis Δ_θ, in region 12 RSL paths are shorter than LSR paths.

So region 13 is optimal for paths of type LSR and region 12 is optimal for paths of type RSL.

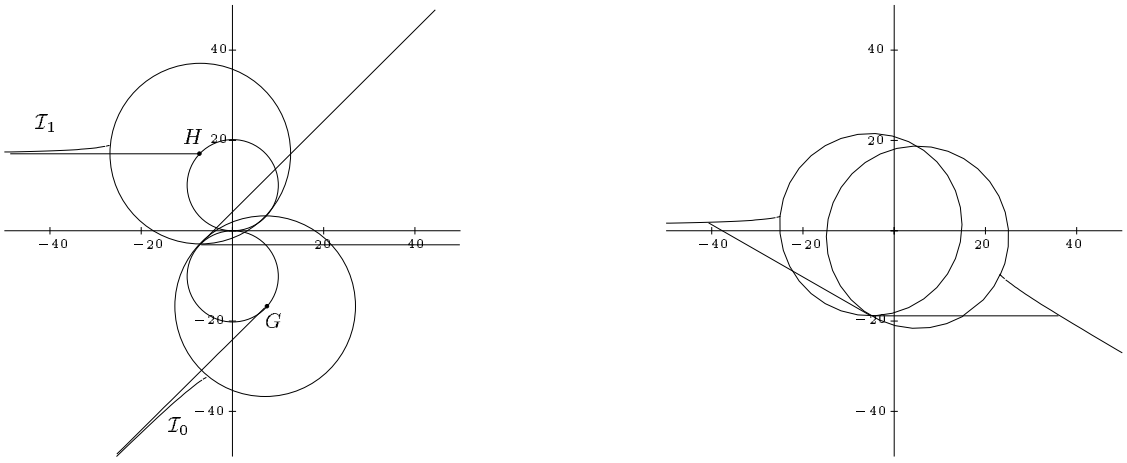

Figure 17: Frontier between types RSR et RSL for $\theta = \pi/4$ (left) and $\theta = 5\pi/6$ (right)

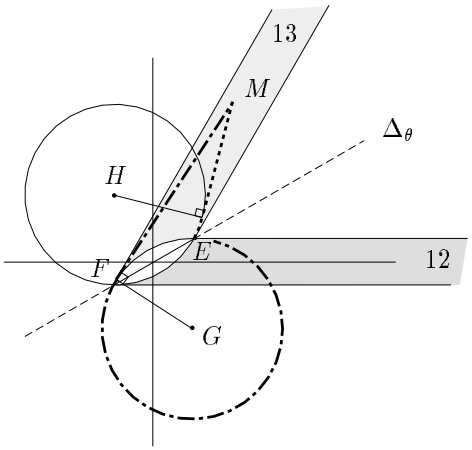

Figure 18: Lengths of RSL and LSR paths in region 13

3.4.3 Intersection *RSR* / *RLR*

This intersection is much simpler and concerns the parts of the discs $\mathcal{C}_G$ and $\mathcal{C}_H$ in the external angular sector defined by D_2 and D_3 (regions 2, 4, 3 and 5). We find geometrically that the set of points reachable from ω_0 by two paths of types RSR and RLR of the same lengths are on a circle called $calI_2$ of radius $4\rho\eta$ and centre F (see Figure 19).

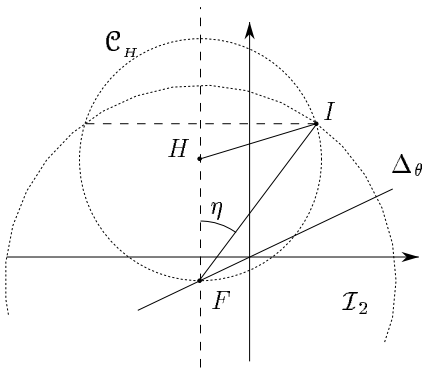

Figure 19: Bounds for arc $calI_2$ inside $\mathcal{C}_H$

Thus the intersection is made of two arcs of the circle $calI_2$ defined by the intervals of polar angles : $[\max(\theta, \pi/2 - \eta), \min(\theta, \pi/2 + \eta)]$ and its symmetric interval w.r.t. $\theta/2$. This intersection occurs only if $\theta \leq \pi/2 + \eta$ (see Figure 20).

3.4.4 Intersection *RLR* / *LRL*

This intersection occurs in regions 4, 5, 8, 9 and 10. The same kind of analysis as for the first intersection case leads to the conclusion that in the intersections between the discs $\mathcal{C}_G$ and $\mathcal{C}_J$, $\mathcal{C}_H$ and $\mathcal{C}_K$, RLR paths are always shorter than LRL paths. But in the intersection of the discs $\mathcal{C}_G$ and $\mathcal{C}_H$ and only for $\theta > \pi/2$, the two types are separated by a curve called $calI_3$ (see Figure 21). After a change of variables due to the rotation of angle $\theta/2$, we obtain the following parametric equations for $calI_3$:

$$calI_3 \begin{cases} X &= \rho \, \dfrac{\cos v + \cos(v+\theta)}{\sin \frac{\theta}{2}} \\ Y^2 &= (4\rho \, \sin \frac{v}{2})^2 - (X - 2\rho \sin \frac{\theta}{2})^2 \end{cases}$$

where v is the length of the intermediate arc of the LRL path. See [Bui94] for the interval in which v varies.

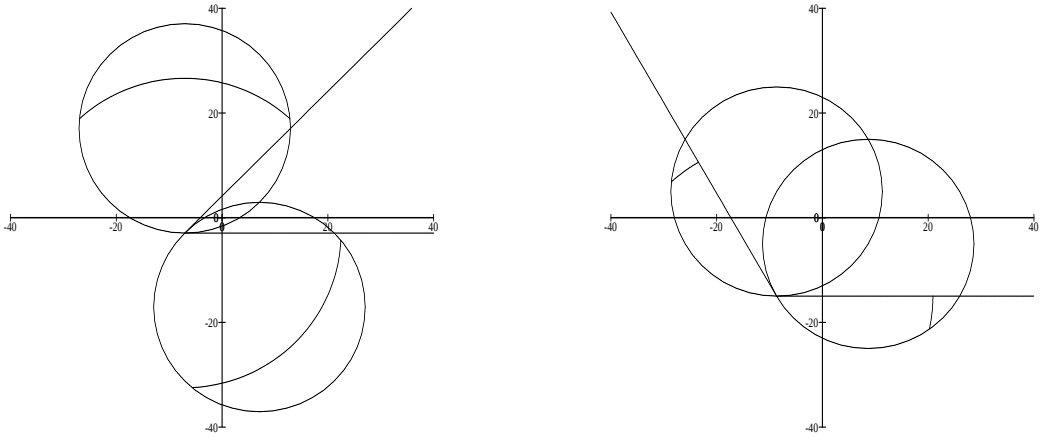

Figure 20: Frontier between RSR and RLR for $\theta = \pi/4$ (left) and $\theta = 2\pi/3$ (right)

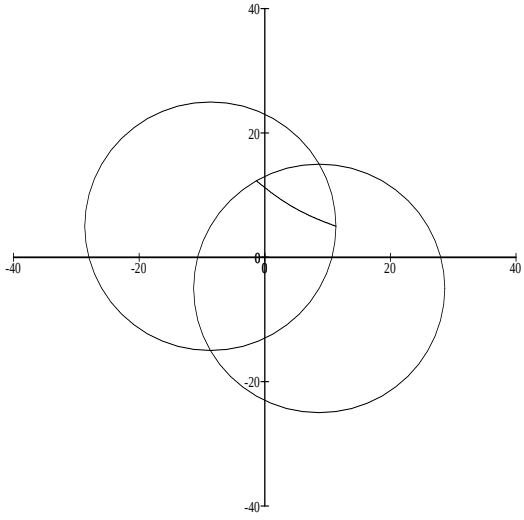

Figure 21: Frontier between RLR et LRL for $\theta = 2\pi/3$

3.4.5 Intersection RLR / RSL

This last intersection separates types RLR and RSL in the region of the disc $\mathcal{C}_H$ which is outside $\mathcal{C}_G$ and in the internal angular sector defined by D_2 and D_3 (regions 7 and 9). We find, with the same method, a curve called $calI_4$, and its symmetric $calI_5$ for the intersection between RLR and LSR (see Figure 22). The parametric equations are the following :

$$calI_4 \begin{cases} x = 2\rho\,(\,\sigma\cos v + \sin v\,) + \rho\sin\theta \\ y = 2\rho\,(\,\sigma\sin v - \cos v\,) - \rho\cos\theta - \rho \end{cases}$$

$$\begin{aligned} \text{with} \quad & v = 2\pi - \arccos\alpha \\ & \alpha = \frac{\sigma^2\,A + B\,\sqrt{4\,(1+\cos\sigma)^2 + 4\,(\sigma+\sin\sigma)^2 - \sigma^4}}{2\,(A^2+B^2)} \\ & A = \cos\theta\,(1+\cos\sigma) - \sin\theta\,(\sigma+\sin\sigma) \\ & B = \cos\theta\,(\sigma+\sin\sigma) + \sin\theta\,(1+\cos\sigma) \end{aligned}$$

where v is the length of the first arc and $2\rho\sigma$ the length of the segment in the RSL paths. We can notice that, here again, we obtain non-algebraic equations. This intersection only occurs for $\theta \geq \pi/2 - \eta$ and see [Bui94] for the range of σ.

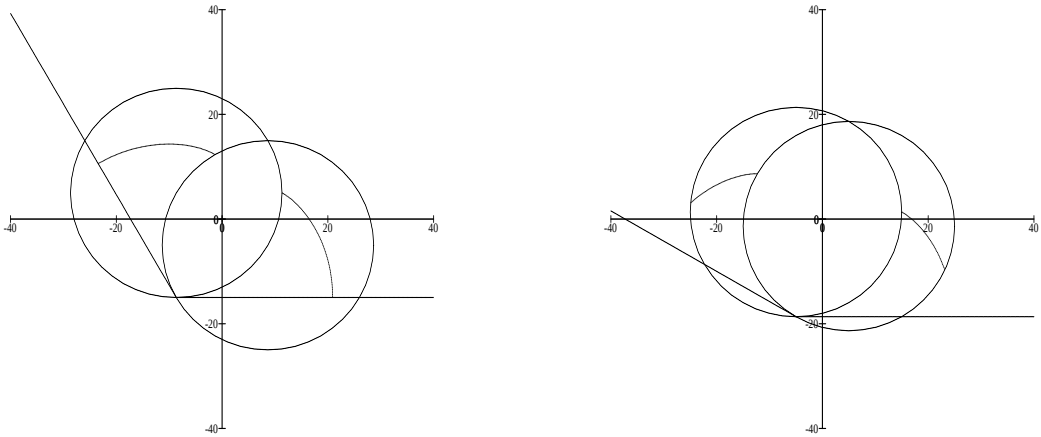

Figure 22: Frontiers between RLR and RSL, and between RLR and LSR, for θ equal to $2\pi/3$ (left) and $5\pi/6$ (right)

4 Results

We finally obtain the partition of P_θ, for any value of θ, taking into account the symmetries and the intersection curves. This partition varies continuously w.r.t. $\theta \in \mathcal{S}^1$, and we can notice four different shapes of partitions, in addition to the particular ones corresponding to $\theta = 0$ and π :

- $\theta = 0$ (Figure 23)

  All types are represented but notice that three regions of the partition are optimal for two types of Dubins path each. Also notice that in fact LRL and LSL domains are not connected : LRL includes also the configuration ω_0, and LSL, the horizontal half-line corresponding to $(x \geq 0, y = 0)$.

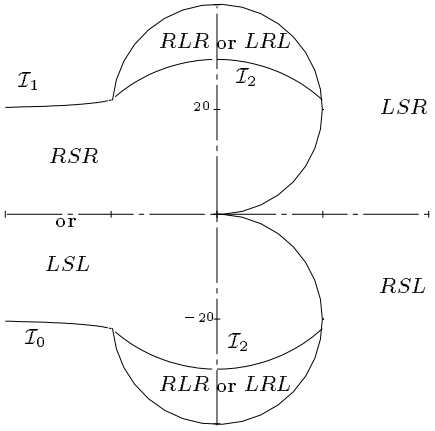

Figure 23: Partition of P_0

- $\theta \in]0, \pi/2 - \eta]$ (Figure 24)

  For $\theta \neq 0$, all regions are optimal for a unique type of path, but some domains are not connected (see RLR, RSL and LSR). At $\theta = \pi/2 - \eta$, the segment of D_2 (*resp.* D_3) and $calI_2$ are intersecting on $\mathcal{C}_G$ (*resp.* $\mathcal{C}_H$).
- $\theta \in]\pi/2 - \eta, \pi/2]$ (Figure 25)

  Here, the intersection curves $calI_4$ and $calI_5$ appear, and at $\theta = \pi/2$ the two crescents of the RLR optimality domain are connected at one point on axis $\Delta_{\pi/2}$.
- $\theta \in]\pi/2, \pi/2 + \eta]$ (Figure 26)

  The intersection curve $calI_3$ has appeared between RLR and LRL. Everything varies continuously until $calI_2$ disappears , at $\theta = \pi/2 + \eta$, since the segment of D_2 (*resp.* D_3), intersection curves $calI_4$ (*resp.* $calI_5$), $calI_0$ (*resp.* $calI_1$) and circle $\mathcal{C}_G$ (*resp.* $\mathcal{C}_H$) are concurrent.

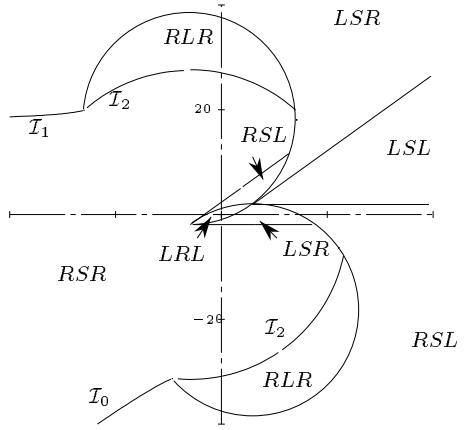

Figure 24: Partition of $P_{\pi/5}$

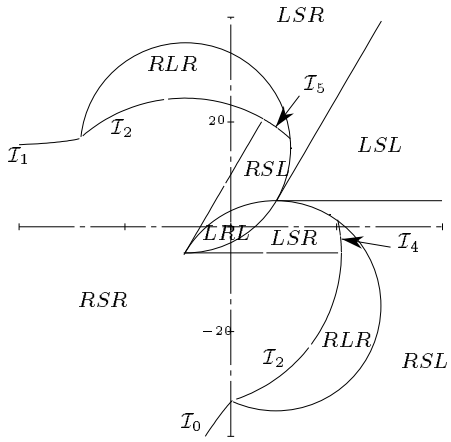

Figure 25: Partition of $P_{\pi/3}$

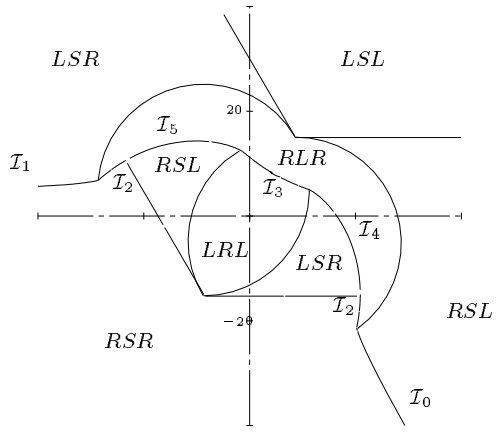

Figure 26: Partition of $P_{2\pi/3}$

- $\theta \in]\pi/2 + \eta, \pi[$ (Figure 27)

  Domains are still varying continuously until $calI_4$ and $calI_5$ disappear, $calI_4$ and $calI_5$ become horizontal half-lines, and $calI_3$ become a horizontal segment of length 4ρ.

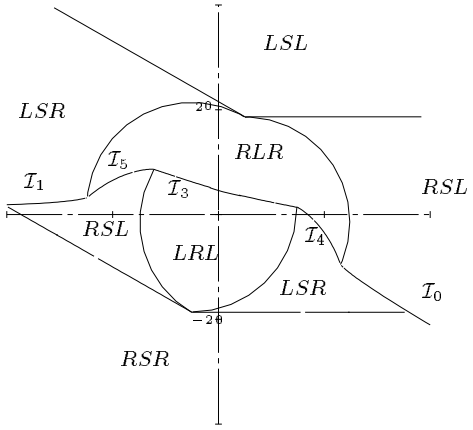

Figure 27: Partition of $P_{5\pi/6}$

- $\theta = \pi$ (Figure 28)

  Now the partition is simple, reduced to the six types with only LSR and RSL domains being non connected.

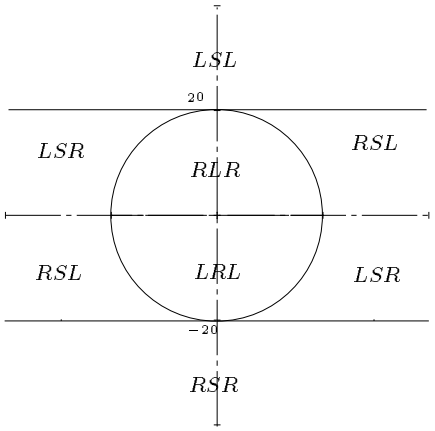

Figure 28: Partition of P_{π}

Moreover, we can emphasize several results :

▷ The optimality domains are not necessarily connected, unlike the Reeds and Shepp case. It is due to the fact that a configuration (x, y, θ) can be reached sometimes in two different ways : either mostly turning left so that the

algebraic sum of angles equals θ, or mostly turning right, then the algebraic sum equals $2\pi - \theta$. In the Reeds and Shepp case, these two solutions cannot cœxist since the algebraic sum of angles has to be less than π.

- ▷ The shape of the shortest paths varies continuously when crossing the boundary of any domain, except the arcs of the boundary of the union of the discs $\mathcal{C}_G$ and $\mathcal{C}_H$, and the intersection curves.

- ▷ The length of the shortest paths is a continuous function of (x, y, θ), except on the arcs of the boundary of the union of discs $\mathcal{C}_G$ and $\mathcal{C}_H$.

  The discontinuities (in shape and length) that occur on the arcs of circles $\mathcal{C}_G$ and $\mathcal{C}_H$ are due to the fact that they are not optimality boundaries for the RSL and LSR paths, but represent conditions of existence : inside the circle $\mathcal{C}_G$ (*resp.* $\mathcal{C}_H$) the RSL (*resp.* LSR) path does not exist.

- ▷ In general, for any point in configuration space, the shortest path is unique. There are two kinds of exceptions. First, on certain boundaries the path type is degenerated so that it can be considered as belonging to two types. For instance, the type SL that is the solution on ray D_0, is degenerated either from type LSL or RSL, which optimality domains are effectively separated by D_0. The second exception is when $\theta \equiv 0\,(2\pi)$, then a whole region can be optimal for two different types, because of Lemma 3.4.

5 Conclusion

This paper has shown how to solve the synthesis problem related to Dubins non-holonomic robot. It has a theoretical interest as a practical application of the Maximum Principle of Pontryagin, since in the general case of optimal control, the synthesis problem remains unsolved. But it is also useful to better understand the motions of such non-holonomic robots. This work has been completed in [Bui94] by the study of the "pseudo-metric" associated to the shortest paths length, and by solving the problem of accessibility, i.e. to find the set of points that can be reached from the origin configuration with an optimal path of length less than or equal to a given value. These results on metric and accessibility, as well as the euclidian distance did for holonomic robots, find a direct application in motion planning for non-holonomic robots.

List of Figures

References

[BCL92] J.-D. Boissonnat, A. Cérézo, and J. Leblond. Shortest paths of bounded curvature in the plane. In *Proc. 9th IEEE Internat. Conf. Robot. Autom.*, 1992.

[Bui94] X-N. Bui. Planification de trajectoire pour un robot polygonal non-holonome dans un environnement polygonal. Thèse de doctorat en sciences, Ecole Nationale Supérieure des Mines de Paris, France, 1994.

[Dub57] L.E. Dubins. On curves of minimal length with a constraint on average curvature and with prescribed initial and terminal positions and tangents. *American Journal of Mathematics*, 79:497–516, 1957.

[PBGM62] L. S. Pontryagin, V. G. Boltyanskii, R. V. Gamkrelidze, and E. F. Mishchenko. *The mathematical theory of optimal processes.* Interscience Publishers, 1962.

[RS90] J.A. Reeds and L.A. Shepp. Optimal paths for a car that goes both forwards and backwards. *Pacific Journal of Mathematics*, 145(2), 1990.

[SL92] P. Souères and J.-P. Laumond. Synthèse des plus courts chemins pour la voiture de Reeds et Shepp. Research Report LAAS/CNRS 92234, LAAS, Toulouse, France, 1992.

[SL93] P. Souères and J.-P. Laumond. Shortest paths synthesis for a car-like robot. In *Second Europeean Control Conference ECC*, Groningen, 1993.

[ST91] H. J. Sussmann and G. Tang. Shortest paths for the Reeds-Shepp car: a worked out example of the use of geometric techniques in nonlinear optimal control. Research Report SYCON-91-10, Rutgers University, New Brunswick, NJ, 1991.

Unité de recherche INRIA Lorraine, Technôpole de Nancy-Brabois, Campus scientifique,
615 rue de Jardin Botanique, BP 101, 54600 VILLERS LÈS NANCY
Unité de recherche INRIA Rennes, IRISA, Campus universitaire de Beaulieu, 35042 RENNES Cedex
Unité de recherche INRIA Rhône-Alpes, 46 avenue Félix Viallet, 38031 GRENOBLE Cedex 1
Unité de recherche INRIA Rocquencourt, Domaine de Voluceau, Rocquencourt, BP 105, 78153 LE CHESNAY Cedex
Unité de recherche INRIA Sophia-Antipolis, 2004 route des Lucioles, BP 93, 06902 SOPHIA-ANTIPOLIS Cedex

Éditeur
INRIA, Domaine de Voluceau, Rocquencourt, BP 105, 78153 LE CHESNAY Cedex (France)
ISSN 0249-6399